applied sciences

MDPI

Article

Influence of Spray Drying on Encapsulation Efficiencies and Structure of Casein Micelles Loaded with Anthraquinones Extracted from *Aloe vera* Plant

Uzma Sadiq *, Harsharn Gill, Jayani Chandrapala * and Fatima Shahid

School of Science, RMIT University, Bundoora, Melbourne, VIC 3083, Australia
* Correspondence: uzma.sadiq@student.rmit.edu.au (U.S.); jayani.chandrapala@rmit.edu.au (J.C.)

Featured Application: Novel spray-dried casein micelles microcapsules were developed to extend the stability and bioavailability of anthraquinones extracted from Aloe vera. These microcapsules can be used commercially in food formulations (yoghurt, bakery products and health drinks) while developing functional foods and nutraceuticals to use as laxative, antibacterial, antiviral and anti-inflammatory.

Abstract: The encapsulation efficiency (EE%) and structural changes within the Anthraquinones-encapsulated casein micelles (CM) powders were evaluated in this study. For this purpose, the anthraquinone powder extracted from Aloevera, its freeze-dried powder (FDP) and whole leaf Aloe vera gel (WLAG) has been encapsulated in CM through ultrasonication prior to spray dying to produce nanocapsules: CM encapsulated anthraquinone powder (CMAQP), CM encapsulated freeze-dried powder (CMFDP) and CM encapsulated Whole leaf aloe vera gel (CMWLAG). Based on the pH of the solution before drying, CMAQP had the highest EE% following spray drying. However, due to air-interface-related dehydration stresses, SD resulted in a slight decrease in the EE% of anthraquinones (aloin, aloe-emodin, and rhein) in CMAQP. Meanwhile, a significant increase in EE% of CMFDP was observed compared to the aqueous state. According to SEM findings, the particle size of CMAQP was 2.39 μm and ξ-potential of ~−17mV. The CMFDP had a rough fractal surface with large particle sizes and potential of 3.49 μm and ~−11mV respectively. CM deformed, having the least EE% and lowest ξ-potential (−4.5 mV). Spray drying enhances melanoidin formation in CMWLAG, as evidenced by the highest chroma values. The results suggested that EE%, stability, and degree of Maillard reaction are closely linked to the type of anthraquinone encapsulated, the pH of the solution, and the nanostructure of casein micelles during spray drying.

Keywords: casein micelles; spray-drying; anthraquinones; encapsulation efficiency; *Aloe vera*; SEM; FTIR

check for updates

Citation: Sadiq, U.; Gill, H.; Chandrapala, J.; Shahid, F. Influence of Spray Drying on Encapsulation Efficiencies and Structure of Casein Micelles Loaded with Anthraquinones Extracted from *Aloe vera* Plant. *Appl. Sci.* **2023**, *13*, 110. https://doi.org/10.3390/app13010110

Academic Editors: Roberto Anedda and Elena Curti

Received: 28 November 2022
Revised: 20 December 2022
Accepted: 20 December 2022
Published: 22 December 2022

Copyright: © 2022 by the authors. Licensee MDPI, Basel, Switzerland. This article is an open access article distributed under the terms and conditions of the Creative Commons Attribution (CC BY) license (https://creativecommons.org/licenses/by/4.0/).

1. Introduction

Incorporation of various bioactive components into food systems towards enhancing the nutritional properties is an active research area within the functional food and nutraceuticals industry. Directly incorporating these bioactive ingredients into food systems is most times restricted due to their instability under various food processing techniques, thus limiting their industrial applications [1]. In this context, encapsulation is an excellent technique involving integrating these bioactive food components into small capsules [2]. Thus, retaining the bioactive components within a protective wall tends to provide a barrier from extreme processing conditions (heat, moisture, chemical reaction), thereby increasing their stability [3].

The selection of wall material for encapsulation plays a vital role. Casein micelles are the cheapest and most familiar wall material, which possess various properties, such as surface activity, emulsifying, gelling and self-assembling [4]. Casein micelles exhibit flexible

conformations that cause the prolongation of powders rehydration in aqueous solutions, with much slower premature release of encapsulated bioactives [5]. Casein micelles are also stable against various unit operations applied within food processing [6], such as heating, freezing and drying [7]. Most recently, casein micelles were used successfully to protect, α-tocopherol [8], Benzydamine [9], jaboticaba extract [10], blueberry anthocyanin [11], curcumin [12], quercetin [13] and anthraquinones [14].

Several researchers have developed diverse encapsulation techniques to protect the bioactive components in casein micelles by preparing nanoemulsions that enhance bioavailability by increasing the surface area to volume ratio [15–17]. However, spray-drying is one of the most valuable and efficient single-step microencapsulation techniques because it can evaporate water rapidly and maintain a relatively low particle temperature [18]. Furthermore, spray-dried powders have excellent technical properties, such as excellent rehydration capacity, high fluidity, and long shelf life [19]. Spray drying is also beneficial for encapsulating various heat-sensitive food ingredients such as polyphenols, flavonoids, anthocyanins, prebiotics, phytosterols and polysaccharides because of limited temperature rises within the matrix during the drying process [20,21]. The surface of the particles stays wet for most of the drying time, and the local ambient temperature does not exceed the wet-bulb temperature. Ultimately, the structural modification of temperature-sensitive compounds stays limited [22].

Our previous article used ultrasonication to encapsulate anthraquinones extracted from Aloe vera into casein micelles [14]. The study concluded that the incorporation of Anthraquinone powder resulted in the highest encapsulation efficiency and yield as opposed to in cooperation of spray-dried powder of aloe vera (SDP), freeze-dried powder of aloe vera (FDP) and whole leaf aloe vera gel (WLAG) based on the anthraquinones to casein micelles ratio, the structure of the anthraquinone, and pH of the solution. However, using these nanocapsules in liquid form while developing functional foods is unstainable due to their perishability and effect on the product's consistency and texture. Hence, all prepared nanocapsules have been spray dried and powders have been evaluated for possible undesirable changes to casein micelles' color and structure due to the Maillard reaction. The obtained powders must possess better applicability within the food industry due to logistical advantages such as less transport cost, easy handling, and more shelf life. According to that knowledge, this study aimed to dry the encapsulated nanoemulsions through spray-drying to understand the drying effect on the encapsulation efficiency and structure of casein micelles.

Moreover, to date, no study has been conducted to determine the stability of these anthraquinone-encapsulated casein micelle solutions when subjected to spray-drying. Thus, the objective of this study was to evaluate the physical, chemical and micro-structural characteristics of spray-dried anthraquinones (extracted from aloe vera) encapsulated casein micelles via ultrasonication. During spray-drying, color measurements and FTIR techniques were employed to assess the browning index and structural organizations. Furthermore, the encapsulation efficiency of anthraquinone-loaded casein micelles as affected by spray-drying was also determined.

2. Materials and Methods

2.1. Materials

Casein micelles powder was purchased from sigma Aldrich Pty Ltd. (Castle Hill, NSW, Australia). Aloe vera (*Aloe barbadensis*) leaves were collected from Aloe vera Australia (Goodman International, Brisbane, Australia). HPLC-grade methanol was purchased from Sigma Aldrich Pty Ltd. (Castle Hill, NSW, Australia). MilliQ water was used at all times.

2.2. Methods

2.2.1. Rehydration of Casein Micelles

Calculated amounts of casein micelle powder based on the protein percentage were dispersed in MilliQ water to obtain a 2% w/w casein micelle solution and the solution

was vigorously shaken for 30 s at first followed by continuous stirring (300 rpm) by a magnetic stirrer (9 MR Hei-Tec Stirrer + Pt1000 V4A) at a temperature of 50 °C for 1 h. The solution was then stirred further for an additional 3 h at room temperature. Casein micelle solutions were allowed to rehydrate at 4 °C in the refrigerator for one day. On the day of encapsulation, the solutions were stirred and equilibrated at 25 °C.

2.2.2. Preparation of Anthraquinones-Loaded Casein Micelles by Ultrasonication

Anthraquinone powders (AQP), freeze-dried powders (FDP) and whole-leaf aloe vera gels (WLAG) were prepared as previously reported [23]. A weighed amount of AQP, FDP, and WLAG were mixed in casein micelle solutions to obtain 20 mg/mL, 20 mg/mL and 4 mg/mL concentrations, respectively. The encapsulation process was completed by sonicating the casein micelle-anthraquinones mixtures with conditions as described previously (Sadiq et al., 2022b). In brief, sonication was performed for 15 min with 30 s pulse on and 30 s pulse off time using a 20 kHz ultrasound equipment (500 W) operating at 50% amplitude which corresponded to an actual power delivery of 39.74 W.

2.2.3. Spray Drying of Anthraquinone-Loaded Casein Micelles

Spray-dried microcapsules of anthraquinone-loaded casein micelles were prepared using a mini spray-dryer B-290 (BÜCHI Labor Technik AG, Meierseggstrasse 40 Postfach, Flawil, Switzerland) which operated at inlet and outlet temperatures of 160 °C and 70 °C, respectively, as given previously [24] with some modifications. All spray-dried powders were stored in Petri dishes, sealed with parafilm, and kept in a desiccator with dry silica gel.

2.3. Characterization of Physical Properties of Spray-Dried Anthraquinone-Loaded Casein Micelles

2.3.1. Encapsulation Efficiency

The anthraquinones present on the surface of the microcapsules and inside the core of the casein micelles were determined. The amount of surface anthraquinones was determined by adding 0.1 g of spray-dried microcapsules to 4 mL of methanol and vortex mixed for 60 s. Then, this mixture was centrifuged at 30,000× *g* for 5 min to obtain the supernatant. The anthraquinones present inside the casein micelles were determined by the same method as above, although the mixtures were sonicated for 10 min in an ultrasonic bath to ensure the complete release of anthraquinones from the interior of casein micelles.

The recovered supernatants after centrifugation were taken carefully and filtered by a 0.45 µm membrane filter for all samples prior to HPLC analysis, as described in our previous article [14]. In general, stock solutions of 1000 µg/mL and working solutions of mixed standards (aloin, aloe-emodin and rhein) were prepared at concentrations of 5 ppm, 10 ppm, 20 ppm and 40 ppm by diluting the stock solution in a volumetric flask with methanol of were prepared by dissolving in HPLC grade methanol and used as standards. HPLC measurements were performed on an Agilent series1250 infinity gradient HPLC (Agilent Technologies, Santa Clara, CA, USA) equipped with a 600 solvent pump and a C18 reversed-phase packing column (Phenomenex XB-C18, 250 mm × 4.60 mm, 3.6 µm Aeris). Gradient elution was performed at 0.7 mL/min, using a binary mobile phase consisting of water with 1% formic acid (A) and methanol (B). The elution was monitored at 254 nm and the injection volume was 20 µL. The HPLC run started with 20% methanol and increased to 30%, 45% and 60% at 3, 10 and 15 min, respectively. The methanol percentage was increased to 70% at 18 min and maintained for 8 min, followed by a gradual decrease to 60%, 40% and 20% at 30, 32 and 35 min, respectively. A calibration curve was established for each standard as a function of their peak areas. The contents of anthraquinones present in the samples were quantified against the standards. T, which was then analyzed by HPLC after filtering through a 0.45-micron filter. The amount of anthraquinones present inside the core of casein micelles were determined by subtracting the surface-attached anthraquinones and the encapsulation efficiency was determined as below:

The following equation was used to calculate

$$Encapsulation\ eficiency\ (EE\%) = Total\ added\ AQ(\mathrm{mg})\text{–}surface\ attached\ AQ(\mathrm{mg})/Total\ added\ AQ\ (\mathrm{mg}) \times 100 \quad (1)$$

where AQ stands for anthraquinones in mg's that are present per gram of spray dried microcapsules

2.3.2. Zeta Potential and pH Measurements

The zeta potential of spray-dried anthraquinone-loaded casein micelles and controlled CMs were determined using a Malvern Zetasizer (Nano Series, Malvern Instrument Ltd., Worcestershire, UK). To achieve appropriate light scattering, the powdered samples were first diluted by the method given by (Bettersize Instruments Ltd. (2021). According to that 10 mg of spray-dried anthraquinones-loaded casein micelle powder (CM, CMAQP, CMFDP, CMWLAG) was dissolved into 100 mL of distilled water. Dissipation was allowed for 15 min by using a magnetic stirrer, followed by filtration through 0.45 microns. Measurements for zeta potential were conducted at room temperature and repeated at least three times, employing a refractive index of 1.57 for the sample and 1.33 for the dispersant.

As previously done for zeta size measurements, the pH of the spray-dried anthraquinone-loaded casein micelles was recorded by diluting the powder in distilled water. The pH of prepared solutions was recorded using the pH Seven Compact TM S220 (Mettler-Toledo GmbH, Im Langacher, Greifensee, Switzerland).

The particle size of spray-dried powders was measured by scanning electron microscopy (FEI Nova Nano 450 FEG-SEM). The size distribution of particles was measured using the software Image J and analyzed by fitting the histogram using a combination of Lorentzian and Gaussian functions. The average particle size was calculated from the average diameter of 20 microparticles.

2.3.3. Color Measurements

Spray drying might cause thermal degradation of casein micelles. Hence, color measurements were used to evaluate the degree of browning level, as a correlation has been reported between the color intensity and formation of advanced Maillard reaction products during spray-drying [25]. So, the color measurements were carried out using the Chroma Meter CR400 (Konica Minolta Sensing Inc., Osaka, Japan), employing the parameters L^* (lightness), a^* (redness), b^* yellowness) defined in the CIE Lab system as per method given by Zahid et al. [26], [27]. Where L^* is the lightness coordinate ranging from $L^* = 0$ (no reflection for black) to $L^* = 100$ (perfect diffuse reflection for white), describes the light-reflecting of the transmittance capacity of an object. A^* represents red (-100) to green (100) and b^* represents yellow (-100) to blue (100) components. All measurements were taken as an average of at least three points on the center and the periphery of each powder layer 1 cm high. The standard white tile's lightness, redness and yellowness were used as reference (L_s 97.14, a_s 0.075, b_s 2.23). The following equation calculated the total color difference:

$$\Delta E = [(L^*s - L^*c)2 + (a^*s - ac^*)2 + (b^*s - bc^*)2]1/2 \quad (2)$$

where s and c stand for standard and spray-dried casein micelles samples, respectively.

The chroma that defines the degree of color saturation and hie angle (H^*), derived from the two coordinates a^* and b^* were determined by the following equations:

$$C^* = (a^{*2} + b^{*2})^{1/2} \quad (3)$$

$$H = \tan^{-1}(b^*/a^*) \quad (4)$$

2.3.4. Moisture Contents

The moisture of anthraquinone-loaded casein micelle powders was determined following the AOAC method (AOAC, 2000). A precise weight of each spray-dried microcapsule

(about 1 g) in triplicate was placed in pre-weighed crucibles and dried in a hot air oven (Qualtex Universal series 2000, Watson victor Ltd., Brisbane, QLD, Australia). The temperature was set at 102 °C and weighed at different periods until a constant weight was obtained. The moisture content was calculated as a percentage using the following formula:

$$M\% = (W1 - W2)/W1 \times 100 \quad (5)$$

W1 is the sample weight (g) before drying, and W2 is the sample weight after drying.

2.3.5. Scanning Electron Microscopy

Spray-dried anthraquinone-loaded casein micelles were evaluated for microstructure using a high-resolution scanning electron microscope (SEM) FEI Nova Nano 450 FEG-SEM at Monash Centre for Electron Microscopy (MCEM). This technique was employed to observe the surface physical morphology, size and composition of the powdered samples and to visually verify the association of the anthraquinones with a micellar casein structure. Each sample was placed on the conductive adhesive and coated with graphite. The images were obtained at magnifications of 5000× and 10,000×. The acceleration voltage was kept between 5–15 KV.

2.3.6. Fourier Transform Infrared (FTIR) Spectroscopy

FTIR spectroscopy was used to evaluate the change in functional groups of the controlled casein micelles (CMs) and spray-dried anthraquinone-loaded casein micelles. FTIR spectra of the powdered samples were obtained using FTIR (Spectrum two, Perkin Elmer, Australia) furnished with IRWinLab FTIR software. Measurements were taken at 4000–400 cm^{-1} for every sample. Thirty-two scans were performed, and the resolution used was 4 cm^{-1}.

2.3.7. Statistical Analysis

All measurements were performed at least in triplicates, and results were expressed in means ± standard deviation. Statistical differences between treatments were evaluated by one-way analysis of variance (ANOVA) available in software SPSS statistical software (23.0 version, Michigan State University, East Lansing, MI, USA). Duncan's multiple range test was used for mean separation and to define significance differences ($p < 0.05$). Figures were created using Origin Pro 8.0 software (OriginLab Corporation, Northampton, MA, USA).

3. Results and Discussion

3.1. Encapsulation Efficiency of Spray-Dried Anthraquinone-Loaded Casein Micelles

Figure 1 shows the encapsulation efficiency of spray-dried casein micelles loaded with AQ powder (CMAQP), freeze-dried powder (CMFDP) and gel (CMWLAG). The encapsulation efficiencies for spray-dried CMAQP were 88%, 72% and 67% for aloin, aloe-emodin and rhein, respectively. However, our earlier study found that the encapsulation efficiencies for aloin, aloe-emodin and rhein in the solution prior to spray-drying were 99%, 98% and 100%, respectively. It indicated an 11%, 26% and 33% decrease [28] for aloin, aloe-emodin and rhein, respectively. The decrease in encapsulation efficiencies after spray-drying was due to the thermal and air-interface-related stresses. The shear rate imparted on casein micelles resulted in the unfolding and exposing of the hydrophobic core of casein micelles [29] carrying anthraquinones (aloin, aloe-emodin, rhein), causing a decrease in EE%. However, the difference in EE% amongst aloin, aloe-emodin and rhein was due to the difference in hydroxyl groups attached to the C ring of aromatic anthraquinones [28] that makes hydrogen bonds with the carbonyl group of casein micelles. As reported previously, aloin, aloe-emodin and rhein are attached within casein micelles mainly through hydrophobic and hydrogen bonding while in solution [14]. Upon spray-drying, the aloin and aloe-emodin are less affected due to being attached to the hydrophobic core. However, rhein encapsulation efficiency decreased significantly, as hydrogen bonds

are weak bonds and easily breakdown by thermal and dehydration stresses during spray-drying and some of these got attached to the surface of casein micelles, as evidenced by Figure 1b.

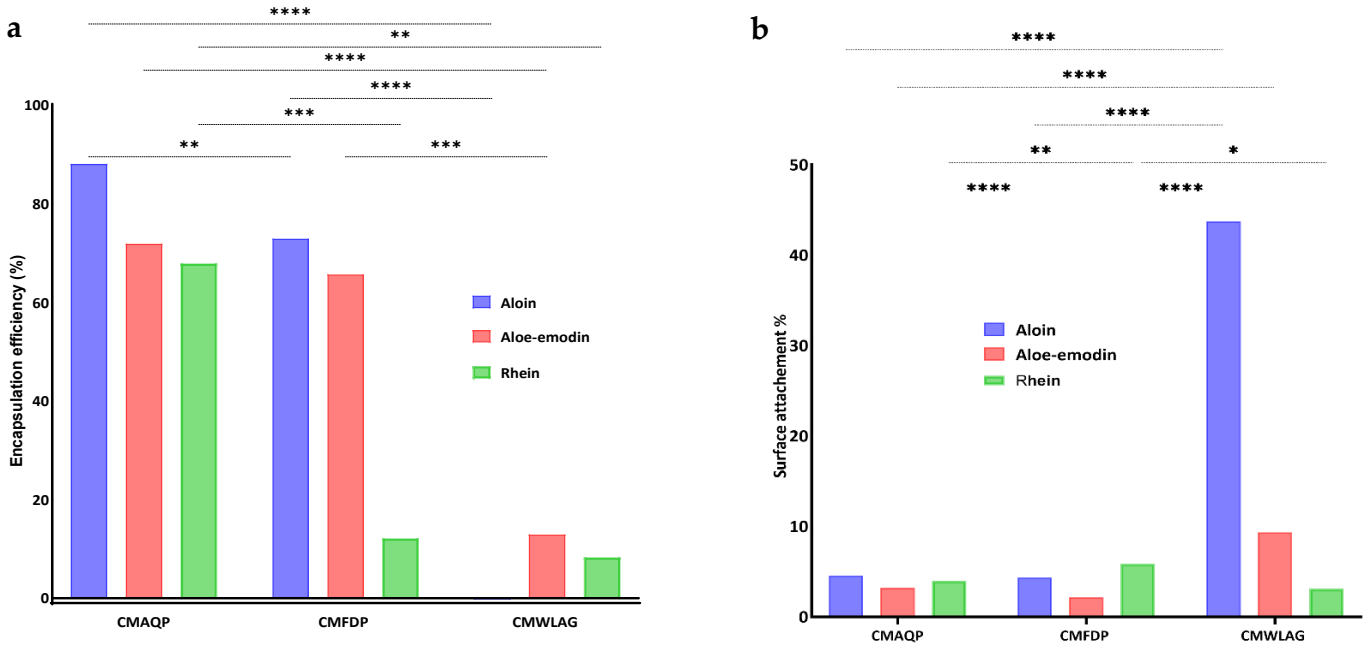


Figure 1. Encapsulation efficiencies (EE%) of anthraquinone-loaded casein micelles (CMAQP, CMFDP, CMWLAG) (**a**) and percentage of surface attachment of anthraquinones (**b**). (Values are from triplicates; the mean and standard deviation are shown. Values significantly different of all spray-dried powders (CMAQP, CMFDP, CMWLAG) when analyzed by two-way ANOVA with Dunnett's test analysis indicated with asterisks: * $p < 0.01$, ** $p < 0.001$, *** $p < 0.0003$, **** $p < 0.0001$.).

Anthraquinone-loaded-casein micelles from freeze-dried powder (CMFDP) exhibited encapsulation efficiencies of 73%, 65% and 12% for aloin, aloe-emodin and rhein, respectively. In the solution phase, 100% of aloe-emodin was encapsulated only before spray-drying, and no aloin nor rhein was encapsulated into casein micelles [14]. The reason is that while in solution form, the aloin started to degrade quickly into aloe-emodin and rhein and could not be detected in the supernatant after centrifugation as per protocol in the previous study [14]. However, aloin and rhein encapsulation efficiency rose to 73% and 12% with spray-drying, respectively. So, the encapsulation efficiency of aloin increased from zero to 73% due to the relocation of free anthraquinones to the inner cluster of casein micelles, as spray-drying caused exposure of embedded hydrophobic regions of casein micelles. After spray-drying, the encapsulation efficiency of aloe-emodin decreased by almost 35%. This decrease in EE% was due to the unavailability of binding sites of casein micelles, which had already been saturated by aloin, as bulky compounds (higher molecular weight) have more affinity to bind with proteins [30] due to more bond formations. While spray-drying, the hydrophobic core of casein micelles gets exposed and could strengthen the interaction between anthraquinones and casein micelles. However, spray-drying did not modify the type of significant interactions [28]. The surface-attached aloin, aloe-emodin and rhein could be calculated in Figure 1b.

The least EE (%) was observed in spray-dried anthraquinone-loaded casein micelles from whole leaf aloe vera gel (CMWLAG) with only 12% aloe-emodin, 8% rhein encapsulated with no aloin being encapsulated. However, according to our previous study, 98% of aloin was encapsulated in the solution phase [14]. This decrease in powder is because of two reasons: Firstly, the decomposition of aloin after harvesting and during extraction in methanol into its degraded isomers, aloe-emodin and rhein, as reported in the previous article [23]. Secondly, during spray-drying, the remaining aloin after decomposition has not

been encapsulated inside the casein micelles; instead started to get attached to the surface of the powders due to its steric hindrance and hydrophilic nature. Hence, aloin shows zero EE%; however, 50% of surface attachment percentage as per Figure 1b while in powdered form. The increase in encapsulation efficiencies of aloe-emodin and rhein from zero to 12% and 8%, respectively, was due to the cluster deformation of casein micelles during spray-drying that could expose the hydrophobic core that facilitated the attachment of aloe-emodin and rhein. However, the least encapsulation efficiency in CMWLAG compared to CMAQP, CMFDP was since, during nanoencapsulation, the pH of the WLAG encapsulated casein micelle (CMWLAG) solution decreased to pH 4.6. The aggregation of casein micelles occurred at their isoelectric point (pI 4.6) and precipitated. These aggregated and fractal structures of CM as a result of acidification, have lower densities [31]. So casein micelles (CMWLAG) maintain weaker, hollow and branched structures [32] that can then easily be broken down by spray-drying [33]. As reported previously, this type of structure is unsuitable for maintaining encapsulated anthraquinones' stability in dried form. Thus, an increase in the free anthraquinones attaching to the hydrophilic terminal instead of attaching to the casein micelles' hydrophobic core (surface attachment as per Figure 1b) decreased the encapsulation efficiencies.

3.2. Zeta Potential and pH of Spray-Dried Anthraquinone-Loaded CMs

Figure 2 shows the zeta−potential of spray-dried casein micelles controlled, CM loaded with AQ powder (CMAQP), freeze-dried powder (CMFDP) and whole leaf Aloe vera gel (CMWLAG). The spray-dried casein micelles were negatively charged with a zeta potential of −17.2 mV. These results were consistent with previous studies [11] where casein micelles' ξ-potential was −16.77 mV after spray-drying [34]. The ξ-potential of CMAQP (−15.4 mV) significantly decreased compared to controlled CMs (−17.2 mV). The difference in zeta potential corresponds to a drop in the pH of controlled casein micelles from 7.4 to 6 after making complexes with anthraquinones, as shown in Table 1. This decrease in ξ−potential of CMAQP due to the shift in pH (from 7.4–5.5) is most probably caused by two pathways. Firstly, the disruption of hairy κ− casein layer and dissociation of some of the calcium phosphate results in rapid aggregation of casein micelles while encapsulating anthraquinones inside the hydrophobic core of the CMs while in the aqueous state [35]. Secondly, during spray-drying, hydrophobic layers of casein micelles are exposed to interact with aloin, aloe-emodin and rhein and form casein-anthraquinone through a well-known protein-phenolic interaction [36] during spray-drying. As reported previously, calcium ions act as bridges between casein micelles [37]; hence, the casein–calcium complex formation through ionic interaction makes it challenging for glucose to bind amine groups of casein, ultimately limiting glycation. The less negative zeta potential limits the formation of negatively charged intermediates during the Maillard reaction; hence a reduction in the glycation of casein micelles was observed. These results aligned with encapsulation efficiency and color parameters, confirming the early stage of the Maillard reaction. However, a decrease in ξ-potential indicates a decrease in casein micelles stability. These results fall between the previously reported ξ-potential of curcumin load nanocapsules where pectin is coated on the surface of casein micelles [12].

In contrast to zeta potential changes of CMAQP, spray-dried CMFDP and CMWLAG showed the highest decreases in zeta potential. CMFDP and CMWLAG resulted in ξ-potential values of −11.2 and −7.5 mV, respectively. As previously reported, the magnitude of ξ-potential increased as the pH decreased [33]. In our previous studies, the pH of casein micelles (CMFDP) decreased from 7.4 to 4.9 [14]. This decrease in pH in CMFDP caused a destabilization of κ-casein, causing the precipitation of casein micelles by releasing some calcium and phosphate ions into the solution. These precipitated CM was unable to hold anthraquinones efficiently while in solution. However, during spray-drying, the anthraquinones attached to the CMs via hydrogen bonding, while in an aqueous solution state, started to attach to the hydrophobic core of the casein micelles through folding and unfolding phenomena causing a reduction in negative charge. Moreover, some an-

thraquinones bound electrostatically to the hydrophilic terminal, causing a decrease in zeta potential. This could be confirmed by comparing the encapsulation efficiencies and surface attachment percentages after spray-drying.

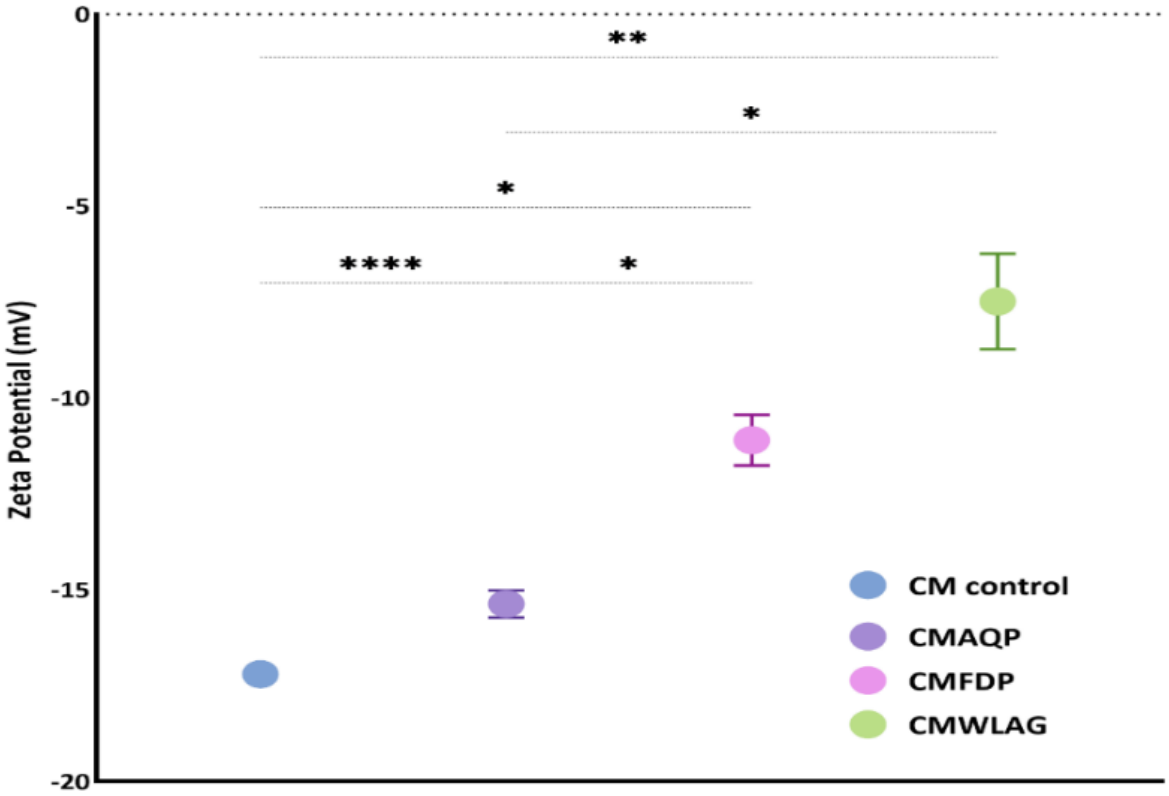


Figure 2. Zeta−potential of spray-dried powders of controlled casein micelles (CMs), CMAQP, CMFDP, and CMWLAG. (Values are from triplicates; the mean and standard deviation are shown. Values significantly different of all spray-dried powders (CMAQP, CMFDP, CMWLAG) from CMs controlled when analyzed by one−way ANOVA with Dunnett's test analysis indicated with asterisks: * $p < 0.01$, ** $p < 0.001$, **** $p < 0.0001$.).

The ξ-potential of casein micelles in the case of CMWLAG was −7.5 mV (Figure 2). This is primarily due to the decrease in pH. The decrease in zeta potential corresponds to a decrease in pH (7.4–4.6), where coagulation and flocculation of casein micelles occur by decreasing the net charge and solubilization of calcium phosphate. As the pH is close to the isoelectric point, the CM is capable of self-assembling and aggregating due to the loss of electrostatic repulsion among them [38]. These aggregated particles start to precipitate when the pH drops to 4.6. During spray-drying, these precipitated CMs bind anthraquinones on its hydrophilic terminal of casein micelles, as evidenced by encapsulation efficiency and structural modification as per FTIR spectra of casein micelles (detailed in FTIR section).

Moreover, the increase in temperature during spray-drying may exert advanced glycation of caseins through glyoxal formation. This could be evident from the color measurement of CMWLAG with the highest chroma value and by FTIR (absence of amide bands). These results contradicted previous findings [38], where a decrease in negative charge was observed upon encapsulation of celecoxib.

Table 1. Moisture contents, pH, color, and visual observations of spray-dried powders of anthraquinone-loaded casein micelles. (Values are mean and standard deviations from triplicate data. The data were analyzed using one-way ANOVA and Tukey's post hoc HSD tests. The different letters in superscript (a, b, c, d) within rows indicate statistically significant differences ($p < 0.05$).

Sample	Moisture (% in Dry Weight)	pH	L^*	a^*	b^*	C^* (Chroma)	H^* (Hue Angle)	ΔE	Visual Observation
CM Control	5.11 ± 0.61^{b}	7.30 ± 0.00^{a}	96.88 ± 0.66^{a}	-0.13 ± 0.02^{d}	3.51 ± 0.81^{c}	3.50 ± 0.80^{c}	92.81 ± 0.34^{a}	1.32^{d}	
CMAQP	4.45 ± 0.40^{c}	5.54 ± 0.02^{b} AQP (5.50)	82.85 ± 0.69^{b}	5.52 ± 0.32^{b}	10.81 ± 0.44^{b}	12.13 ± 0.53^{b}	63.29 ± 0.82^{c}	17.54^{c}	
CMFDP	5.91 ± 0.23^{b}	4.87 ± 0.12^{b} FDP (4.52)	79.75 ± 1.37^{c}	7.7 ± 0.53^{a}	9.44 ± 0.25^{b}	12.19 ± 0.53^{b}	50.79 ± 1.22^{d}	20.32^{b}	
CMWLAG	6.50 ± 0.81^{a}	4.65 ± 0.00^{c} WLAG (4.56)	73.03 ± 0.58^{d}	4.79 ± 0.07^{c}	22.32 ± 0.29^{a}	22.82 ± 0.27^{a}	77.88 ± 0.27^{b}	31.73^{a}	

3.3. Colour and Moisture Contents of Spray-Dried Anthraquinone-Loaded Casein Micelles

The color of a food product is the principal factor determining its quality attributes and consumer preferences. The color measurements of spray-dried controlled casein micelles (CMs) and anthraquinone-loaded casein micelles (CMAQP, CMFDP, CMWLAG) determined using CIE L^* a^* b^* system are given in Table 1.

In general, the lightness of controlled casein micelles (CMs) L^* was 96.88 ± 0.66, and a significant decrease ($p < 0.05$) was observed in anthraquinone-loaded casein micelles (CMAQP), where L^* was 82.85 ± 0.69 (Table 1). This significant decrease in the luminosity of CMAQP may have been caused by the early stage of the Maillard reaction depending upon anthraquinones being encapsulated, which might act as a catalyst and could modify the reaction pathway during spray-drying [39]. Throughout the early stage of the Maillard reaction, the Schiff bond formation occurs between amino acids of casein micelles and sugars of anthraquinones to produce protein-bonded Amadori products, as reported previously [40] and these are less brown and are most stable. This has been confirmed by encapsulation efficiencies and zeta potential measurements. Similarly, the parameter a^* in anthraquinone-loaded casein micelles increased significantly from -0.13 ± 0.0 to 5.52 ± 0.32 (CMAQP) with spray-drying, which was also an indication of Maillard reaction as reported previously in liquid milk and infant formula [41]. The parameter b^* increased from 3.51 ± 0.81 (CM control) to $10.81 \pm 0.44'$ showing an increase in yellowness after spray-drying which suggested an increase in yellow components of the color that is consistent with a decrease in L^* and visual assessment (Table 1).

The CMFDP showed L^*, a^* and b^* with an average value of 79.75 ± 1.37, 7.7 ± 0.53, and 9.44 ± 0.25, respectively. The advanced stage of the Maillard reaction may have caused a decrease in lightness during spray-drying, depending upon the nature of the sample

being encapsulated. The parameter a^* in CMFDP changed significantly after spray-drying with an average value of 4.79 ± 0.07, respectively, which reflects more significant redness. The yellowness b^* changed CMFDP and was highest in CMWLAG with an average of 22.32 ± 0.29.

The CMWLAG showed lightness with an average value of 73.03 ± 0.58. The lowest L^* was due to the formation of a brown pigment called melanoidins produced as a result of the final stage of the Maillard reaction [42] and the highest b^* corresponds to increased redness and increased yellowness of the spray-dried Aloe vera powder [43] as compared to casein micelles. These results agreed to the previous studies, where curcumin-doped casein micelles were prepared through spray-drying [44] and a decrease in lightness and an increase in yellowness indicated the browning process as depicted by visual assessment.

Chroma *(C*)* values are indicative of overall saturation which varies from dull at low chroma values to vivid color at high chroma values [45]. The controlled casein micelles possess a chroma value of 3.50 ± 0.80, indicating very low color saturation, so the powder appears white [44]. The chroma values of CMAQP and CMFDP were 12.13 ± 0.5 and 12.19 ± 0.5 (Table 1) respectively, corresponding to early Maillard reaction products in CMAQP and advanced glycation in the case of CMFDP. In CMAQP, the anthraquinones might limit the early glycation of casein micelles by forming more favorable quinones under these pH conditions (5.5). The anthraquinones-loaded CMAQP and CMFDP appeared less saturated in color, which corresponds to the binding of anthraquinones inside the hydrophobic core of the CMs and early and advanced stage of Maillard reaction as evidenced by encapsulation efficiency and zeta potential. The chroma value for CMWLAG was 22.82, representing the more intense yellowish color due to melanoidins. These results are consistent with previously reported chroma values of spray-dried reconstituted skim milk [46]. In addition, the highest chroma value in CMWLAG corresponds to the more structural changes of casein micelles and accumulation of anthraquinones on the hydrophilic terminal as a result of spray-drying and the final stage of Maillard reactions, as shown in Table 1. These changes in chroma values of the samples are similar to the trend observed previously to measure the extent of the Maillard reaction based on the fluorescence of tryptophan and advanced Maillard reaction products' AMP/Trp ratio [25].

The hue angle value is the measure of the degree of the color circle, which ranges from 0 to 360 degrees, red-purple at angle 0°, yellow at 90°, bluish-green at 180° and blue at 270°. The hue angle of the controlled CMs was 92.81 ± 0.34, which means it should be yellow to green; nevertheless, its low chroma C^* value of 3.50 ± 0.80 explains a very low color saturation; hence the powder appears white. The CMWLAG presents a hue angle H^* of 77.88 ± 0.27, followed by CMAQP (63.29 ± 0.82) and CMFDP (50.79 ± 1.22) correspond to yellow and slightly red as these values indicated that the colors of the anthraquinone-loaded casein micelles were between red (0°) and yellow (90°) as per color quadrant [47].

Standalone L^* a^* and b^* values are not sufficient to describe the colors of powders. The overall color change is given by color difference (ΔE^*_{ab}) in terms of spatial distance between two color points and has been used to describe the color of powdered samples in other studies [45] as all spray-dried anthraquinone-loaded casein micelles have $\Delta E > 1.5$. This difference described the degree of browning due to the Maillard reaction during spray-drying while encapsulating anthraquinones [48] into casein micelles as a result of spray-drying. Overall, all spray-dried anthraquinone-loaded-casein micelles exhibited low moisture contents ranging from 4.45–6.50% (<5.50%), which contributed to their high storage stability [19]. The water retained in the spray-dried casein micelles during spray-drying may be due to the water binding capacity of casein micelles and the degree of Maillard reaction. Regarding CMAQP, it exhibited the lowest moisture content with an average of 4.45 ± 0.4. This decrease in moisture contents compared to spray-dried controlled casein micelles was due to the incorporation of anthraquinones (aloin, aloe-emodin, rhein) that interact firmly within casein micelles while displacing water molecules

during spray-drying. These results aligned with encapsulation efficiencies and the smallest microstructure of CMAQP.

The CMWlAG had the highest moisture content with an average amount of 6.50 ± 0.8 due to water molecules and the condensation mechanism between the amino group of casein micelles and the carbonyl group of sugars containing aloin. Moreover, the water retained in casein micelles during spray-drying might be due to the water binding capacity of CMs, as evident from the lowest encapsulation efficiencies and larger microstructure of CMWLAG. Even so, these values were in line with other studies that reported the moisture content of spray-dried powders to be up to 7.5% [49–51]. Moreover, these results were consistent with previous results (5%; [52]), where milk powders were used to encapsulate curcumin under the same spray-drying parameters. This leads to the conclusion that spray-dried powder presents lower moisture contents at higher inlet temperatures [20], which was also concluded from the present study.

3.4. Comparison of Microcapsules by Scanning Electron Microscopy (SEM)

Scanning electron microscopy images of the freshly produced CMs and CMAQP, CMFDP, and CMWLAG are shown in (Figure 3A–D). The SEM image of control CMs (Figure 3A1a,A2a) reveals the typical morphology of spray-dried casein micelles composed of spherical particles with a shrunken and essentially smooth surface. As controlled casein micelles have been spray dried after rehydration, the micrographs of controlled casein micelles (Figure 3A1a,A2a) depicting the short bridges and direct inter-micellar contacts that act together to maintain a casein micelles network, hence, resist disruption into individual caseins after spray-drying [53]. These micrographs were also consistent with previously reported CM structures after spray-drying [11]. Some holes and roughness on the surface of casein micelles were visible with a wrinkled and deflated morphology with open voids, as described previously [54,55]. The wrinkled particles were related to the low diffusion coefficients of caseins. As the droplets dried before casein molecules diffused evenly, dimpled particles were formed.

Figure 3B1b,B2b showed the morphology of CMAQP having wrinkled and non-spherical shapes. It can be explained that anthraquinones should have been bound to casein and embedded in the hydrophobic location of casein micelles after encapsulation. κ-caseins and β-casein quickly separated from a micellar structure at lower pH (5.5) and lower temperature, respectively. However, as the temperature rises during spray-drying, β-caseins reincorporate. This suggests that the structure was entirely open at pH 5.5, allowing for the incorporation of anthraquinones while displacing water molecules and retained inside the casein micelles during spray-drying, giving non-spherical casein micelles with irregular and rough surfaces. The incorporation of AQ into casein micelles (Silva et al., 2015) was supported by Figure 3B2b, which depicted fibril-like casein micelles adhering to one another (as depicted by 20 μm image) with non-micellar material serving as glue. According to our previous study, this non-micellar substance might be β-caseins separated from casein micelles in solution [14], which has been attached to the surface of the powder.

Additionally, the solvent evaporation and molecular diffusion ratios when anthraquinones are added to CMs change the shape of CMAQP. The particle size of CMAQP (2.39 ± 1.1 μm) microcapsules was less than the control casein micelles (2.65 ± 0.93 μm; [11]), showing encapsulation of AQ within casein micelles' hydrophobic core by displacing water molecules from the interior of casein micelles. It can also be confirmed by low moisture contents, higher encapsulation efficiency and through SEM images, where CM shape and appearance changed from spherical to non-spherical and irregular objects with tiny dimples, which might lead to the incorporation of anthraquinones into the interior of casein micelles. These results are consistent with shapes already given in literature while making coffee-casein complexes and spray-dried emodin-casein microcapsules [56,57].

Figure 3C1c,C2c shows the morphology of CMFDP having rough, fractal surfaces. A change in protein to minerals ratio causes the loosening and swelling of casein micelles [58,59]. As before spray-drying, the measured pH of the solution was 4.9, where

solubilization of some colloidal calcium phosphate takes place. Casein micelles would eventually aggregate during spray-drying due to the breakage of hydrogen bonding that held anthraquinones inside and outside the micelles. Moreover, at this pH, the mean intra-particle distance increases and the probability of finding a next-neighbor particle at a specific distance decrease. So, the obtained CMs were fractal with a rough surface and the production of a cluster after spray-drying for CMFDP was larger than the reassembled CMs. The particle size of CMFDP was 3.46 ± 1.2 µm which suggests that CMFDP were fractal with rough surfaces and are the cluster prepared by an aggregation system that was larger in diameter prepared from the reassembled system. The swelling of casein micelles also corresponds to high moisture contents, as described in the previous section.

Figure 3D1d,D2d) shows the morphology of casein micelles while encapsulating WLAG (CMWLAG). CMWLAG produced a cluster with randomly growing branches in stilliform geometry and a few spherical, smooth surface particles corresponding to Aloe vera. The reason is that casein micelles are aggregated by acidification while in an aqueous state. These aggregated casein micelles enlarge in size during spray-drying, causing casein micelles to loosen and perhaps swell. The causes of this are the pH, salt content, and dehydration-related stressors that expose the hydrophobic areas during spray-drying and cause them to lose their structural integrity [60,61]. The smaller particle size (2.57 ± 1.2 µm) than the controlled casein micelles suggest the precipitation of casein micelles by acidification with the exclusion of water. The particle size results were consistent with previous literature [9].

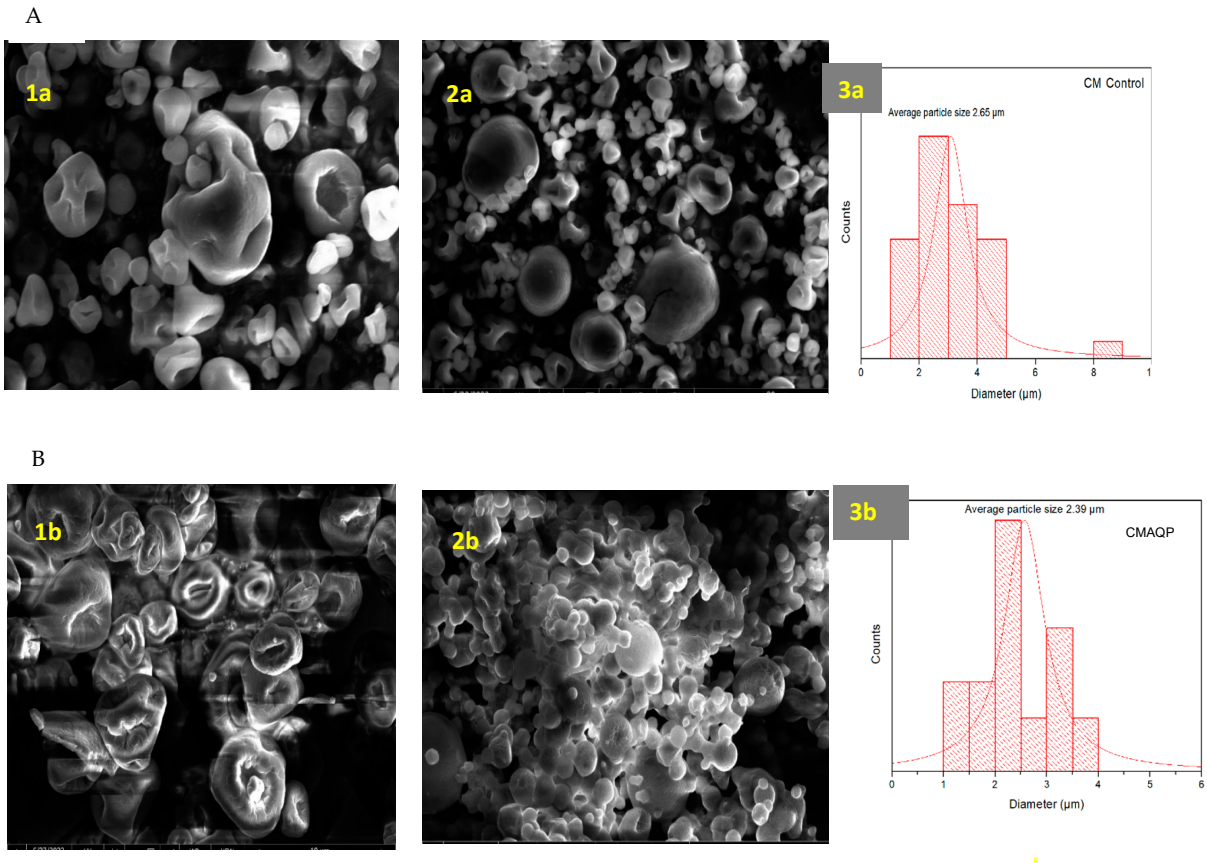


Figure 3. *Cont.*

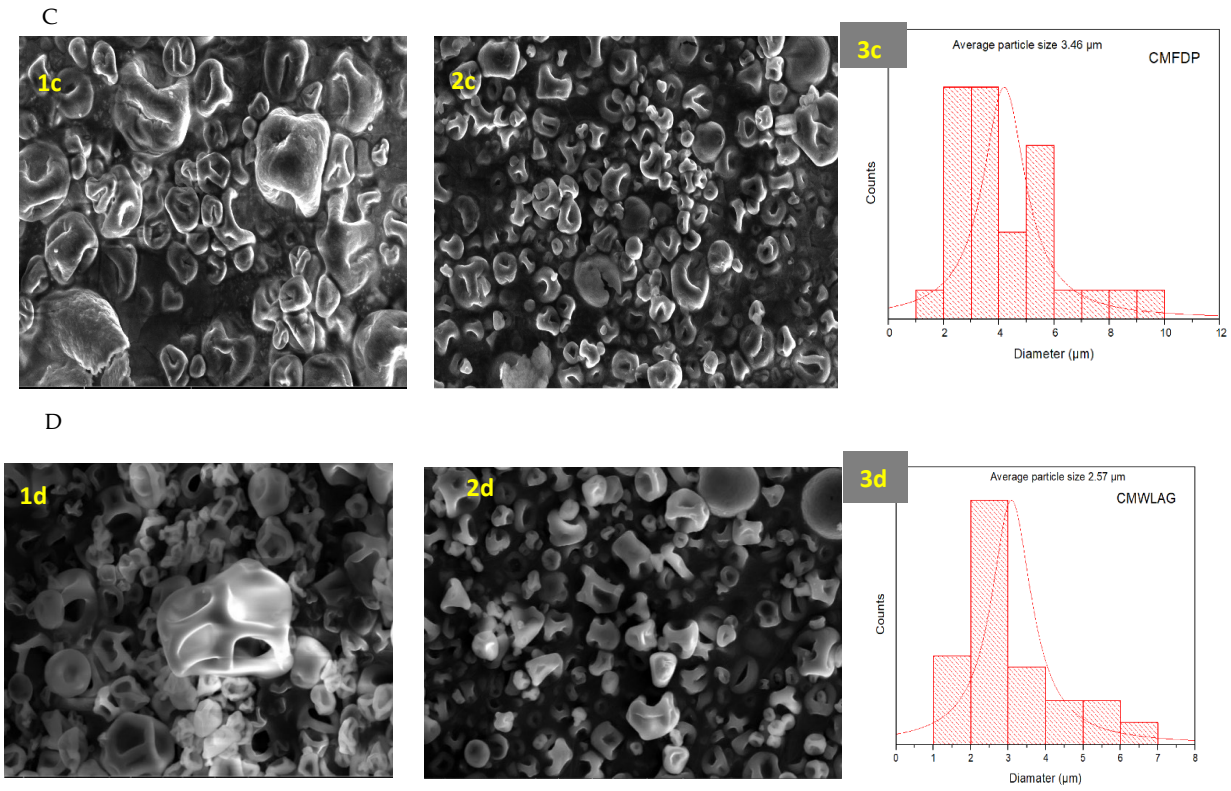


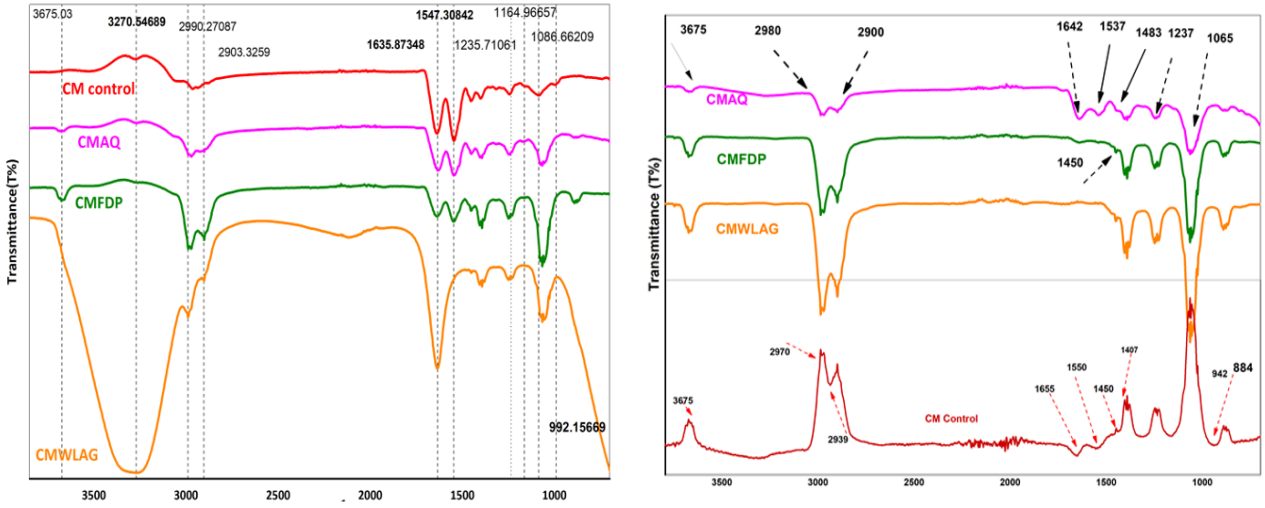
Figure 3. Scanning electron micrographs of freshly produced powders of CM controlled (**A**), CMAQP (**B**), CMFDP (**C**), and CMWLAG (**D**). Photographs (**1a–1d**) were taken originally using a magnification of 10,000×, and the scale bar 10 µm scale, Photographs (**2a–2d**) were originally taken using a magnification of 5000× and the scale bar 20 µm, (**3a–3d** represent particle size distribution of CM control, CMAQP, CMFDP and CMWLAG, respectively).

3.5. FTIR

FTIR has been used to compare the secondary structure of the anthraquinone-loaded casein micelles (CMAQP, CMFDP, CMWLG) before and after spray-drying, as shown in Figure 4a,b. The controlled casein micelles (CMs) and anthraquinone-loaded casein micelles (CMAQP, CMFDP, CMWLAG) showed altered bands both in frequencies and intensities before (a) and after spray-drying (b). Generally, the FTIR spectra of casein micelles (Figure 4a,b) showed peaks for amide A band (3280–3225 cm^{-1}), amide I (1700–1600 cm^{-1}) amide II (1450–1550 cm^{-1}) and amide III (1350–1200 cm^{-1}) bands [62]. The discreetly intense peak near 1086 cm^{-1} and 1065 cm^{-1} can be related to phosphate stretching of colloidal calcium phosphate [63].

Spray drying of CMAQP shifted the amide I and amide II bands to higher and lower energy levels, respectively, as shown in Figure 4b. Before spray-drying, amide I bands were located at 1635 cm^{-1} (Figure 4a), however, the amide I peak shifted from 1635 from 1642 cm^{-1} after spray-drying. This shift to higher energy can be attributed to the shrinkage of protein structure upon spray-drying. The shifting in amide II bands in CMAQP Figure 4a towards lower energy from 1547 to 1537 cm^{-1} indicates that upon spray-drying, the casein micelles have relaxed with a broader range of conformational geometry. These spectral changes are consistent with previous studies and can be attributed to the loosening and shrinkage of protein structure due to spray-drying. A change in intensities at 2980 and 2969 cm^{-1} after spray-drying in CMQP corresponds to hydrophobic interactions [64], suggesting the methyl stretching of aliphatic chains of anthraquinones. These hydrophobic interactions are due to the accommodation of anthraquinones on hydrophobic regions of casein micelles after spray-drying that was attached to CM through hydrogen bondings while in solution. The secondary structure of casein micelles remained

unchanged in CMAQP after spray-drying, suggesting the therapeutic effectiveness and functional properties of spray-dried anthraquinone-loaded casein micelles. The peak at 1065 cm^{-1} after spray-drying in CMAQP corresponds to CCP due to rapid aggregation of CMs after spray-drying, which was absent before spray-drying in CMAQP.



(**a**) (**b**)

Figure 4. FTIR spectra of controlled casein micelles (CM control) and spray-dried microcapsules of CMAQP, CMFDP, and CMWLAG before (**a**) [14] and after spray-drying (**b**).

Regarding CMFDP (Figure 4b), the disappearance of amide I and amide II bands at 1641 and 1537 cm^{-1}, respectively, after spray demonstrated deformation of the casein micelle's structure due to folding and unfolding of casein micelles. Even before spray-drying (Figure 4a) in CMFDP, these bands are present at 1635 and 1545 cm^{-1}. This suggests that the secondary structure of casein micelles had been altered after drying.

The strong peaks at 1065 cm^{-1} in CMFDP after spray-drying (Figure 4b) correspond to calcium-casein complexes after the Maillard reaction that coated the surface of aggregated and reassembled casein micelles. However, these peaks were absent in the aqueous phase suggesting the absence Maillard reaction.

Regarding CMWLAG, both amide I and amide II bands vanished after spray-drying. However, before spray-drying, a change in the amide II band and disappearance of amide I can be observed. The sharp peaks at 1065 cm^{-1} in CMWLAG before spray-drying (Figure 4a) correspond to calcium phosphate liberation due to acid-induced precipitation of CMs [59]. However, after spray-drying, the peak intensity enhanced, suggesting the coating of calcium ions on the powdered surface. The disappearance of amide I and II bands after spray-drying corresponds to the denaturation of casein micelles due to heat, dehydration and interface indued stresses during spray-drying, as previously reported [58].

4. Conclusions

In this study, anthraquinone-loaded casein micelles were developed successfully by ultrasonication, and nano capsule solidification was carried out using spray-drying.

- Spray drying caused a decrease in encapsulation efficiencies of aloin, aloe-emodin and rhein in CMAQP due to the shear rate imparted on casein micelles due to dehydration stress and temperature.
- In contrast, CMFDP exhibited increased EE% of aloin and rhein due to the accessibility of an embedded hydrophobic binding site after spray-drying and got attached to the core of casein micelles by folding and unfolding of CM structure, as evident by FTIR.
- A decrease in zeta potential, particle size and lightness corresponded to an early stage of Maillard reaction during spray-drying in CMAQP, while spray-drying did not

change the secondary structure of casein micelles in CMAQP. However, the secondary structure of casein micelles altered in CMFDP and CMWLAG due to air-interface stresses during spray-drying as a result of the pH of nano capsules.
- The color parameters of CMAQP, CMFDP and CMWLAG, corresponded to the early, advanced and final stages of the Maillard reaction, respectively. These results suggested that encapsulation efficiencies depend on pH, spray-drying conditions, and degree of Maillard reaction.

Author Contributions: U.S.: Conceptualization, Methodology, Investigation, Formal analysis, Software, Data curation, Validation and Writing—original draft., H.G.: Writing—review and editing, Supervision, Methodology, Validation, Funding acquisition, Resources J.C.: Writing—review and editing, Supervision, Methodology, Software, Data Curation and Validation. F.S.: Methodology, Formal analysis. All authors have read and agreed to the published version of the manuscript.

Funding: This research received no external funding.

Institutional Review Board Statement: Not applicable.

Informed Consent Statement: Not applicable.

Data Availability Statement: The data presented in this study are available on request from the corresponding author.

Acknowledgments: We are thankful to the Higher Education Commission (HEC) of Pakistan and RMIT University, Australia, for supporting our scholarship.

Conflicts of Interest: The authors declare no conflict of interest.

References

1. Chopde, S.; Datir, R.; Deshmukh, G.; Dhotre, A.; Patil, M. Nanoparticle formation by nanospray drying & its application in nanoencapsulation of food bioactive ingredients. *J. Agric. Food Res.* **2020**, *2*, 100085.
2. Nedovic, V.; Kalusevic, A.; Manojlovic, V.; Levic, S.; Bugarski, B. An overview of encapsulation technologies for food applications. *Procedia Food Sci.* **2011**, *1*, 1806–1815. [CrossRef]
3. Labuschagne, P. Impact of wall material physicochemical characteristics on the stability of encapsulated phytochemicals: A review. *Food Res. Int.* **2018**, *107*, 227–247. [CrossRef] [PubMed]
4. Sadiq, U.; Gill, H.; Chandrapala, J. Casein Micelles as an Emerging Delivery System for Bioactive Food Components. *Foods* **2021**, *10*, 1965. [CrossRef] [PubMed]
5. Ji, J.; Fitzpatrick, J.; Cronin, K.; Maguire, P.; Zhang, H.; Miao, S. Rehydration behaviours of high protein dairy powders: The influence of agglomeration on wettability, dispersibility and solubility. *Food Hydrocoll.* **2016**, *58*, 194–203. [CrossRef]
6. Malekhosseini, P.; Alami, M.; Khomeiri, M.; Esteghlal, S.; Nekoei, A.R.; Hosseini, S.M.H. Development of casein-based nanoencapsulation systems for delivery of epigallocatechin gallate and folic acid. *Food Sci. Nutr.* **2019**, *7*, 519–527. [CrossRef]
7. Shapira, A.; Assaraf, Y.G.; Livney, Y.D. Beta-casein nanovehicles for oral delivery of chemotherapeutic drugs. *Nanomed. Nanotechnol. Biol. Med.* **2010**, *6*, 119–126. [CrossRef]
8. Sun, L.; Wang, H.; Li, X.; Lan, S.; Wang, J.; Yu, D. Ultrasonic-assisted preparation of α-Tocopherol/casein nanoparticles and application in grape seed oil emulsion. *Ultrason. Sonochem.* **2021**, *80*, 105810. [CrossRef]
9. Zahariev, N.; Marudova, M.; Milenkova, S.; Uzunova, Y.; Pilicheva, B. Casein Micelles as Nanocarriers for Benzydamine Delivery. *Polymers* **2021**, *13*, 4357. [CrossRef]
10. Nascimento, L.G.L.; Casanova, F.; Silva, N.F.N.; de Carvalho Teixeira, Á.V.N.; Júnior, P.P.D.S.P.; Vidigal, M.C.T.R.; Stringheta, P.C.; de Carvalho, A.F. Use of a crosslinked casein micelle hydrogel as a carrier for jaboticaba (*Myrciaria cauliflora*) extract. *Food Hydrocoll.* **2020**, *106*, 105872. [CrossRef]
11. Liao, M.; Ma, L.; Miao, S.; Hu, X.; Liao, X.; Chen, F.; Ji, J. The in-vitro digestion behaviors of milk proteins acting as wall materials in spray-dried microparticles: Effects on the release of loaded blueberry anthocyanins. *Food Hydrocoll.* **2021**, *115*, 106620. [CrossRef]
12. Hua, C.; Yu, W.; Yang, M.; Cai, Q.; Gao, T.; Zhang, S.; Xu, H.; He, H.; Peng, N.; Liu, Y. Casein-pectin nanocomplexes as a potential oral delivery system for improving stability and bioactivity of curcumin. *Colloid Polym. Sci.* **2021**, *299*, 1557–1566. [CrossRef]
13. Chen, C.; Chen, Z.; Zhong, Q. Caseinate nanoparticles co-loaded with quercetin and avenanthramide 2c using a novel two-step pH-driven method: Formation, characterization, and bioavailability. *Food Hydrocoll.* **2022**, *129*, 107669. [CrossRef]
14. Sadiq, U.; Gill, H.; Chandrapala, J. Ultrasound-Assisted Encapsulation of Anthraquinones Extracted from Aloe-Vera Plant into Casein Micelles. *Gels* **2022**, *8*, 597. [CrossRef]
15. Lee, W.J.; Tan, C.P.; Sulaiman, R.; Smith Jr, R.L.; Chong, G.H. Microencapsulation of red palm oil as an oil-in-water emulsion with supercritical carbon dioxide solution-enhanced dispersion. *J. Food Eng.* **2018**, *222*, 100–109. [CrossRef]

16. Wandrey, C.; Bartkowiak, A.; Harding, S.E. Materials for encapsulation. In *Encapsulation Technologies for Active Food Ingredients and Food Processing*; Springer: Berlin/Heidelberg, Germany, 2010; pp. 31–100.
17. Lucas, J.; Ralaivao, M.; Estevinho, B.N.; Rocha, F. A new approach for the microencapsulation of curcumin by a spray drying method, in order to value food products. *Powder Technol.* **2020**, *362*, 428–435. [CrossRef]
18. Rigon, R.T.; Zapata Noreña, C.P. Microencapsulation by spray-drying of bioactive compounds extracted from blackberry (*Rubus fruticosus*). *J. Food Sci. Technol.* **2016**, *53*, 1515–1524. [CrossRef]
19. Nikolova, Y.; Petit, J.; Gianfrancesco, A.; Sanders, C.F.W.; Scher, J.; Gaiani, C. Impact of Spray-Drying Process Parameters on Dairy Powder Surface Composition and Properties. *Dry. Technol.* **2015**, *33*, 1654–1661. [CrossRef]
20. Fang, Z.; Bhandari, B. Effect of spray drying and storage on the stability of bayberry polyphenols. *Food Chem.* **2011**, *129*, 1139–1147.
21. Ray, S.; Raychaudhuri, U.; Chakraborty, R. An overview of encapsulation of active compounds used in food products by drying technology. *Food Biosci.* **2016**, *13*, 76–83. [CrossRef]
22. Filková, I.; Mujumdar, A.S. Industrial spray drying systems. In *Handbook of Industrial Drying*; CRC Press: Boca Raton, FL, USA, 2020; pp. 263–307.
23. Sadiq, U.; Gill, H.; Chandrapala, J. Temperature and pH Stability of Anthraquinones from Native Aloe vera Gel, Spray-Dried and Freeze-Dried Aloe vera Powders during Storage. *Foods* **2022**, *11*, 1613. [CrossRef] [PubMed]
24. Bastías-Montes, J.M.; Choque-Chávez, M.C.; Alarcón-Enos, J.; Quevedo-León, R.; Muñoz-Fariña, O.; Vidal-San-Martín, C. Effect of spray drying at 150, 160, and 170 C on the physical and chemical properties of maqui extract (*Aristotelia chilensis* (Molina) Stuntz). *Chil. J. Agric. Res.* **2019**, *79*, 144–152. [CrossRef]
25. Zhou, Z.; Langrish, T. Color formation and Maillard reactions during the spray drying process of skim milk and model systems. *J. Food Process Eng.* **2022**, *45*, e13936. [CrossRef]
26. Zahid, H.F.; Ranadheera, C.S.; Fang, Z.; Ajlouni, S. Utilization of mango, apple and banana fruit peels as prebiotics and functional ingredients. *Agriculture* **2021**, *11*, 584. [CrossRef]
27. Zahid, H.F.; Ranadheera, C.S.; Fang, Z.; Ajlouni, S. Functional and Healthy Yogurts Fortified with Probiotics and Fruit Peel Powders. *Fermentation* **2022**, *8*, 469. [CrossRef]
28. Xu, H.; Lu, Y.; Zhang, T.; Liu, K.; Liu, L.; He, Z.; Xu, B.; Wu, X. Characterization of binding interactions of anthraquinones and bovine β-lactoglobulin. *Food Chem.* **2019**, *281*, 28–35. [CrossRef]
29. Maa, Y.F.; Hsu, C.C. Protein denaturation by combined effect of shear and air-liquid interface. *Biotechnol. Bioeng.* **1997**, *54*, 503–512. [CrossRef]
30. Hasni, I.; Bourassa, P.; Hamdani, S.; Samson, G.; Carpentier, R.; Tajmir-Riahi, H.-A. Interaction of milk α-and β-caseins with tea polyphenols. *Food Chem.* **2011**, *126*, 630–639. [CrossRef]
31. Bremer, L.G.; van Vliet, T.; Walstra, P. Theoretical and experimental study of the fractal nature of the structure of casein gels. *J. Chem. Soc. Faraday Trans. 1 Phys. Chem. Condens. Phases* **1989**, *85*, 3359–3372. [CrossRef]
32. Chardot, V.; Banon, S.; Misiuwianiec, M.; Hardy, J. Growth kinetics and fractal dimensions of casein particles during acidification. *J. Dairy Sci.* **2002**, *85*, 8–14. [CrossRef]
33. Jarunglumlert, T.; Nakagawa, K.; Adachi, S. Influence of aggregate structure of casein on the encapsulation efficiency of β-carotene entrapped via hydrophobic interaction. *Food Struct.* **2015**, *5*, 42–50. [CrossRef]
34. Anema, S.G.; Klostermeyer, H. ζ-Potentials of casein micelles from reconstituted skim milk heated at 120 C. *Int. Dairy J.* **1996**, *6*, 673–687. [CrossRef]
35. Creamer, L.K.; Plowman, J.E.; Liddell, M.J.; Smith, M.H.; Hill, J.P. Micelle Stability: κ-Casein Structure and Function. *J. Dairy Sci.* **1998**, *81*, 3004–3012. [CrossRef]
36. Akıllıoğlu, H.G.İ.; Gokmen, V. Effects of hydrophobic and ionic interactions on glycation of casein during Maillard reaction. *J. Agric. Food Chem.* **2014**, *62*, 11289–11295. [CrossRef]
37. Krishnankutty Nair, P. Colloidal Behaviour of Casein Micelles with Concentration. Ph.D. Thesis, University of Guelph, Guelph, ON, Canada, 2012.
38. Bachar, M.; Mandelbaum, A.; Portnaya, I.; Perlstein, H.; Even-Chen, S.; Barenholz, Y.; Danino, D. Development and characterization of a novel drug nanocarrier for oral delivery, based on self-assembled β-casein micelles. *J. Control. Release* **2012**, *160*, 164–171. [CrossRef]
39. Zhong, C.; Tan, S.; Langrish, T. Redness generation via Maillard reactions of whey protein isolate (WPI) and ascorbic acid (vitamin C) in spray-dried powders. *J. Food Eng.* **2019**, *244*, 11–20. [CrossRef]
40. Van Boekel, M. Effect of heating on Maillard reactions in milk. *Food Chem.* **1998**, *62*, 403–414. [CrossRef]
41. Morales, F.; Van Boekel, M. A study on advanced Maillard reaction in heated casein/sugar solutions: Colour formation. *Int. Dairy J.* **1998**, *8*, 907–915. [CrossRef]
42. Bosch, L.; Alegría, A.; Farré, R.; Clemente, G. Fluorescence and color as markers for the Maillard reaction in milk–cereal based infant foods during storage. *Food Chem.* **2007**, *105*, 1135–1143. [CrossRef]
43. Kumar, N. Optimization of spray drying conditions for production of aloe-vera powder. *Chem. Sci. Rev. Lett.* **2017**, *6*, 525–532.
44. Khanji, A.N.; Michaux, F.; Petit, J.; Salameh, D.; Rizk, T.; Jasniewski, J.; Banon, S. Structure, gelation, and antioxidant properties of curcumin-doped casein micelle powder produced by spray-drying. *Food Funct.* **2018**, *9*, 971–981. [CrossRef] [PubMed]
45. Hunter, R.S.; Harold, R.W. *The Measurement of Appearance*; John Wiley & Sons: Hoboken, NJ, USA, 1987.

46. Nijdam, J.; Langrish, T. An investigation of milk powders produced by a laboratory-scale spray dryer. *Dry. Technol.* **2005**, *23*, 1043–1056. [CrossRef]
47. McLellan, M.; Lind, L.; Kime, R. Hue angle determinations and statistical analysis for multiquadrant Hunter L, a, b data. *J. Food Qual.* **1995**, *18*, 235–240. [CrossRef]
48. Horvath, Z.H.; Halasz-Fekete, M. Instrumental colour measurement of paprika grist. *Ann. Fac. Eng. Hunedoara* **2005**, *3*, 101–106.
49. Learoyd, T.P.; Burrows, J.L.; French, E.; Seville, P.C. Chitosan-based spray-dried respirable powders for sustained delivery of terbutaline sulfate. *Eur. J. Pharm. Biopharm.* **2008**, *68*, 224–234. [CrossRef]
50. Carter, B.; Patel, H.; Barbano, D.M.; Drake, M. The effect of spray drying on the difference in flavor and functional properties of liquid and dried whey proteins, milk proteins, and micellar casein concentrates. *J. Dairy Sci.* **2018**, *101*, 3900–3909. [CrossRef]
51. Corrigan, O. Thermal analysis of spray dried products. *Thermochim. Acta* **1995**, *248*, 245–258. [CrossRef]
52. Neves, M.I.L.; Desobry-Banon, S.; Perrone, I.T.; Desobry, S.; Petit, J. Encapsulation of curcumin in milk powders by spray-drying: Physicochemistry, rehydration properties, and stability during storage. *Powder Technol.* **2019**, *345*, 601–607. [CrossRef]
53. Mimouni, A.; Deeth, H.C.; Whittaker, A.K.; Gidley, M.J.; Bhandari, B.R. Rehydration process of milk protein concentrate powder monitored by static light scattering. *Food Hydrocoll.* **2009**, *23*, 1958–1965. [CrossRef]
54. Dalgleish, D.G. On the structural models of bovine casein micelles—Review and possible improvements. *Soft Matter* **2011**, *7*, 2265–2272. [CrossRef]
55. Sadek, C.; Schuck, P.; Fallourd, Y.; Pradeau, N.; Jeantet, R.; Le Floch-Fouere, C. Buckling and collapse during drying of a single aqueous dispersion of casein micelle droplet. *Food Hydrocoll.* **2016**, *52*, 161–166. [CrossRef]
56. Tan, S.; Ebrahimi, A.; Langrish, T. Smart release-control of microencapsulated ingredients from milk protein tablets using spray drying and heating. *Food Hydrocoll.* **2019**, *92*, 181–188. [CrossRef]
57. Yang, M.; Wei, Y.; Ashokkumar, M.; Qin, J.; Han, N.; Wang, Y. Effect of ultrasound on binding interaction between emodin and micellar casein and its microencapsulation at various temperatures. *Ultrason. Sonochem.* **2020**, *62*, 104861. [CrossRef]
58. Singh, H. Interactions of milk proteins during the manufacture of milk powders. *Le Lait* **2007**, *87*, 413–423. [CrossRef]
59. McKenna, A.B. Effect of Processing and Storage on the Reconstitution Properties of Whole Milk and Ultrafiltered Skim Milk Powders: Thesis Presented in Partial Fulfilment of the Requirement for the Degree of Doctor of Philosophy in Food Technology. Ph.D. Thesis, Massey University, Palmerston North, New Zealand, 2000.
60. Cleland, J.L.; Powell, M.F.; Shire, S.J. The development of stable protein formulations: A close look at protein aggregation, deamidation, and oxidation. *Crit. Rev. Ther. Drug Carr. Syst.* **1993**, *10*, 307–377.
61. Wolkers, W.F.; van Kilsdonk, M.G.; Hoekstra, F.A. Dehydration-induced conformational changes of poly-L-lysine as influenced by drying rate and carbohydrates. *Biochim. Biophys. Acta (BBA)-Gen. Subj.* **1998**, *1425*, 127–136. [CrossRef]
62. Li, Y.; Zhang, X.; Sun, N.; Wang, Y.; Lin, S. Formation and evaluation of casein-gum arabic coacervates via pH-dependent complexation using fast acidification. *Int. J. Biol. Macromol.* **2018**, *120*, 783–788.
63. Holt, C.; WAHLGREN, M.N.; DRAKENBERG, T. Ability of a β-casein phosphopeptide to modulate the precipitation of calcium phosphate by forming amorphous dicalcium phosphate nanoclusters. *Biochem. J.* **1996**, *314*, 1035–1039. [CrossRef]
64. Liu, F.; Ma, D.; Luo, X.; Zhang, Z.; He, L.; Gao, Y.; McClements, D.J. Fabrication and characterization of protein-phenolic conjugate nanoparticles for co-delivery of curcumin and resveratrol. *Food Hydrocoll.* **2018**, *79*, 450–461. [CrossRef]

Disclaimer/Publisher's Note: The statements, opinions and data contained in all publications are solely those of the individual author(s) and contributor(s) and not of MDPI and/or the editor(s). MDPI and/or the editor(s) disclaim responsibility for any injury to people or property resulting from any ideas, methods, instructions or products referred to in the content.